water

MDPI

Article

Energy Transfer from the Freshwater to the Wastewater Network Using a PAT-Equipped Turbopump

Maria Cristina Morani [1,*], Armando Carravetta [1], Oreste Fecarotta [1] and Aonghus McNabola [2]

[1] Department of Civil, Architectural and Environmental Engineering (DICEA) of University of Naples, "Federico II", 80125 Napoli, Italia; arcarrav@unina.it (A.C.); oreste.fecarotta@unina.it (O.F.)

[2] Department of Civil, Structural & Environmental Engineering, Trinity College Dublin, Dublin D02 PN40, Ireland; amcnabol@tcd.ie

* Correspondence: mariacristina.morani@unina.it; Tel.: +39-0817-683453

Received: 11 September 2019; Accepted: 17 December 2019; Published: 20 December 2019

Abstract: A new strategy to increase the energy efficiency in a water network exists using turbo pumps, which are systems consisting of a pump and a turbine directly coupled on a same shaft. In a turbo pump, the pump is fed by a turbine that exploits a surplus head in a freshwater network in order to produce energy for one system (wastewater) and reduce the excess pressure in another (drinking water). A pump as turbine (PAT) may be preferred over a classic turbine here due to its lower cost. The result of such a coupling is a PAT–pump turbocharger (P&P). In this research, the theoretical performance of a P&P plant is employed using data from a real water distribution network to exploit the excess pressure of a freshwater stream and to feed a pump conveying wastewater toward a treatment plant. Therefore, the P&P plant is a mixed PAT–pump turbocharger, operating with both fresh and wastewater. A new method to perform a preliminary geometric selection of the machines constituting the P&P plant has been developed. Furthermore, the plant operation has been described by means of a new mathematical model under different boundary conditions. Moreover, the economic viability of the plant has been assessed by comparison with a conventional wastewater pumping system working in ON/OFF mode. Therefore, the net present value (NPV) of the investment has been evaluated in both situations for different time periods. According to the economical comparison, the PAT–pump turbocharger represents the most economically advantageous configuration, at least until the useful life of the plant. Such convenience amounts to 175% up to a time period equal to 20 years.

Keywords: energy recovery; pump as turbine (PAT); Mixed PAT–Pump turbocharger (MP&P); water distribution network; hydraulic power; wastewater sewage

1. Introduction

Nowadays, one of the main challenges in the water industry consists of the reduction of environmental impacts, as well as the containment of energy use. Water distribution networks are usually low energy efficiency systems, due to the high energy consumption [1], as well as the important amount of water leakage that affects these systems. Indeed, the energy consumption associated with water distribution networks accounts for approximately 2%–3% of worldwide consumption [2]. As regards water leakage, it represents a significant waste of energy [3], leading to consequences for operating costs [4] and environmental impact [5–8]. Cabrera et al. [9] showed that 40%–60% of the total energy spent in water distribution systems is lost due to leakage, flow resistances, and minor losses, due to the geometry of the pipelines.

Sustainable growth [8] in this sector could be achieved through several strategies, which aim at an optimal management of water distribution networks. For example, optimal pump scheduling, in both clean water [10–12] and drainage [13–16] pumping systems has been shown to improve energy efficiency. In particular, a recent study [15] showed that an optimal pump scheduling in a drainage system can ensure an average value of recovered energy up to 32%. It has recently been shown [17] that supplying a reservoir located upstream of a water network and dissipating the excess energy using a hydropower turbine is likely to be preferred over pumping directly to the network, depending on the characteristics of the hydraulic system. Among these energy-saving strategies, the replacement of pressure reducing valves (PRVs) with energy production devices (EPDs) represents one of the most advantageous strategies, which ensures both energy recovery [18] and leakage reduction [19–22].

Since water leakage is strongly related to the pressure in the network, pressure management is needed to decrease the amount of water lost in pipes [23–25]. The use of PRVs to perform such pressure control strategies is common practice [26]; however, these do not allow performing any energy recovery. As an alternative pressure control strategy, EPDs such as micro-hydropower turbines have been highlighted in recent literature, where this excess energy is not dissipated and thus wasted; rather, it is exploited by the devices themselves to produce electricity [27–30].

An innovative strategy for water pumping is represented by turbo-pumps [21], namely, systems consisting of a turbine and a pump that are directly coupled and mounted on the same shaft. The turbine converts the hydraulic power and transfers the mechanical torque to the pump. Such a strategy ensures both the recovery of stream energy and the reduction of pumping energy consumption, increasing the whole efficiency of the hydraulic system. Turbo-pumps can be adopted whenever a storage tank is used within a network to pump water toward an upper part of the grid. The turbine can exploit the excess pressure upstream of the tank to gather power and feed the pump, in order to guarantee sufficient pressure to the users at the higher parts of the network. The excess energy needs to be dissipated, and it could be comparable with the energy required to pump water toward the higher tank. Therefore, a turbine could be located at the tank inflow in order to both reduce pressure and produce energy to supply the pump. Furthermore, in order to reduce equipment costs, a pump as turbine (PAT) [31] could be employed instead of a classic turbine, with acceptable efficiency [32–35], obtaining a PAT–pump turbocharger (P&P). The operating principle, the performance, and the advantages of a P&P plant in a water supply system have been stressed by [21]. Other possible applications may occur in the process industry, where the excess pressure of a process can be used to pump liquids for other purposes.

The aim of this paper consists of analyzing a new strategy to save energy in a water system. In particular, it has adopted the employment of a PAT–pump turbocharger (P&P) to convey wastewater into a treatment plant from a low topographical level. The pumping of this wastewater is achieved from the reduction of pressure in a co-located drinking water network, which requires pressure reduction in supplying water from a higher elevation to this low topographical location. Thus, the new device would be a mixed PAT–pump turbocharger (MP&P), since PAT and pump operate with clean and wastewater, respectively. The mixed PAT–pump turbocharger could be adopted whenever water distribution networks are located in low ground level areas, which hence require pumping stations to carry wastewater to a treatment plant. In particular, this plant arises whenever the wastewater pumping station is required in the same location as an excess clean-water pressure is available. Such situation is not rare, since it can happen whenever the town has a large variability in elevation. In these cases, the highest pressure in the freshwater network occurs where the ground elevation is the lowest, and there, a pressure reducing station is often required to minimize the leakage. In the same areas, due to the need to treat the wastewater, the sewage system is usually equipped with pumping stations, to pump toward the treatment plants. When the energy recoverable by the PAT is small, a conversion to electricity through a PAT/generator would not be convenient, due to the installation costs and the need for connecting the generator to the grid. A direct transfer of the available mechanical power from the PAT shaft to the pump shaft can be more convenient. Another advantage of the MP&P is the simplification

of the mechanic of the plant. Two separate plants operating independently (a hydropower recovery plant with its own generator and a pumping plant with its own motor) apparently exhibit a higher resilience, because a simultaneous failure of the two machines has a low probability. Nevertheless, the absence of electric devices simplifies the mechanic of the plant and could reduce the failure rate as well as the maintenance costs.

In this paper, the main features of the MP&P plant are explained and a new method to perform a preliminary design of the plant, according to both the maximum daily average fresh and sewage discharges, is also presented. Moreover, a new mathematical model describing the plant operation is formulated for different boundary conditions. In addition, an economic comparison with a conventional wastewater pumping system working in ON/OFF mode is carried out. Finally, the limitations of the plant are also investigated.

2. Mixed PAT–Pump Turbocharger Operation

In a mixed PAT–pump turbocharger plant, a PAT is employed to produce energy by exploiting a surplus head, which otherwise would be dissipated through a PRV or into an open tank. Located on the same shaft as the PAT, a pump, rotating at the same rotational speed of the PAT ($N_P = N_{PAT} = N$), exploits the energy recovered by the PAT to carry sewage to a water treatment plant. In this way, the mechanical power is directly transferred from the PAT to the pump ($P_{PAT} = P_P = P$). Therefore, the pump is not supplied by any external electrical motor. In the mixed PAT–pump turbocharger, the pump and PAT can achieve any rotational speed. In spite of this, the rotational speed will result from the combination of the performance curves of the two devices with the network characteristics.

Compared to P&P in freshwater systems [21], the MP&P is characterized by a reduced overall efficiency, since channel or vortex pumps, namely, pumps used for wastewater discharges, are characterized by a lower performance. A simplified scheme of a MP&P plant is presented in Figure 1.

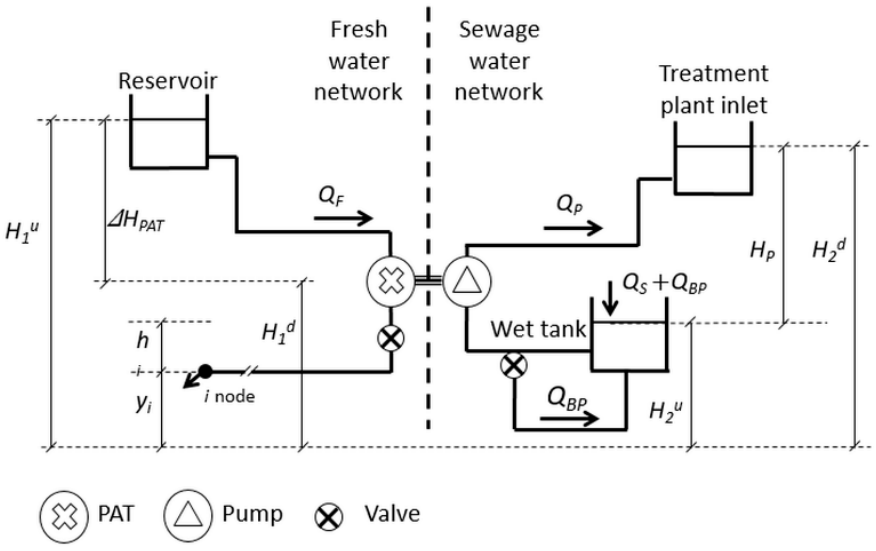

Figure 1. Hydraulic scheme of mixed pump as turbine–pump (MP&P).

According to Figure 1, H_1^u and H_1^d are the head available at the hydropower plant inlet and outlet, respectively; Q_F is the freshwater discharge; ΔH_{PAT} is the head loss within the PAT; Q_S and Q_P are, respectively, the wastewater discharge reaching the wet tank and the discharge pumped to the treatment plant with a hydraulic head equal to H_2^d. In addition, Q_{BP} represents a bypassed discharge. The bypass is placed in order to avoid the emptying of the wet tank: when the pumped discharge is too high, a part of the flow is recirculated to the wet tank. This would prevent damages to the pump due to the suction of air with the additional benefit of mixing of the water volume in the wet well,

avoiding the sedimentation of solid material. Finally, H_P is the pressure head computed with respect to the water level in the tank, namely, H_2^u.

Furthermore, the sewage pumping pipelines are commonly characterized by a short length in order to avoid system blockage; for this reason, head losses can be neglected. Moreover, head losses from the freshwater storage tank to the hydropower plant have been considered negligible as well, due to the shortness of the branch. Further explanations of plant operation are provided in [21]. A deep investigation about the relationship between turbined and pumped discharge, as well as the relationship between pressure head and head loss within the PAT, has been carried out by [21]. Indeed, [21] analyzed different working conditions depending on the number of stages of both the PAT and the pump. In particular, by fixing the number of PAT stages to 1 and increasing the number of pump stages, the range of flow rate ratio Q_P/Q_F decreases while the head ratio $H_P/\Delta H_T$ increases. In addition, according to [21], the efficiency of the P&P system also depends on the number of stages. Indeed, for a number of PAT stages equal to 1, the lowest efficiency is attained for a single-stage pump, whereas it significantly increases (from less than 0.35 up to more than 0.45) by increasing the number of pump stages. [21] also showed that the best efficiency (equal to 0.45) occurred for a three-stage pump.

3. Study Area

The application of the mixed PAT–pump turbocharger has been assessed through its theoretical performance using real-world water network data as a case study. The analyzed case study comprises a drinking water supply network from a rural area, in a small Irish village, located in County Laois, about 100 km from Dublin (IE).

The network is supplied by a reservoir located at 147 m a.s.l. (above sea level), receiving water through a pumping station, from a source placed at 99 m a.s.l. The layout of the water distribution network is shown in Figure 2. For the whole network, information about pipe roughness, diameter, and length was available.

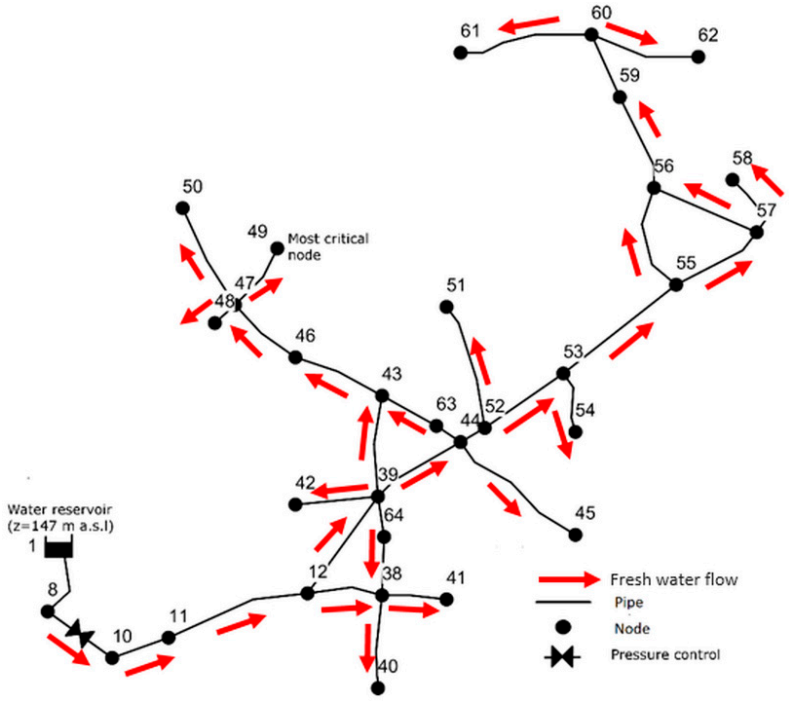

Figure 2. Hydraulic network of the study area (modified from [17]).

As shown in Figure 2, the network is provided with an upstream valve located along the pipe connecting nodes 8 and 10, to perform a pressure control strategy within the network. In Figure 3a, the daily trend of the flow rate in the pipe is presented.

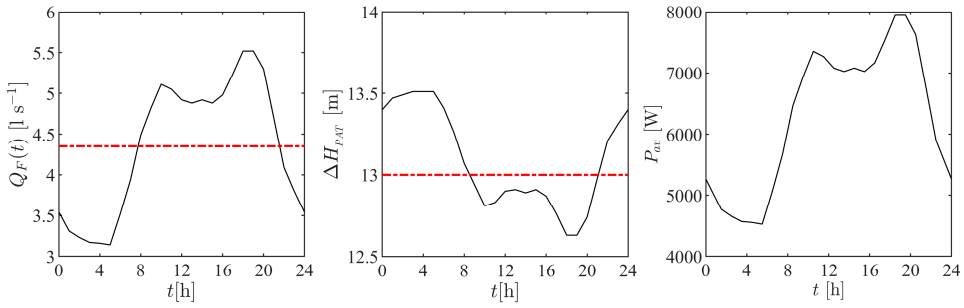

(**a**) (**b**) (**c**)

Figure 3. Time series of flow (**a**) and head loss (**b**) though the valve located in links 8–10 [17], available power (**c**) upstream of the valve.

In previous research [17], the design of a hydropower plant, replacing the pressure reducing valve in the branch between nodes 8 and 10 (Figure 2), has been performed, and the hydraulic behavior of the network has been simulated using Epanet [36]. In particular, the plant has been provided with a PAT configured using hydraulic regulation [37] including a series-parallel hydraulic circuit (Figure 4). This guarantees the provision of a minimum pressure head in all the nodes of the network, and in particular, a pressure of 10 m in the most critical node of the network (node 49). When the head is higher than the head loss deliverable by the PAT, the excess of pressure is dissipated by a series pressure reducing valve (PRV). Instead, if the discharge is larger, a bypass is opened to reduce it, as the PAT would produce a head loss higher than the available head.

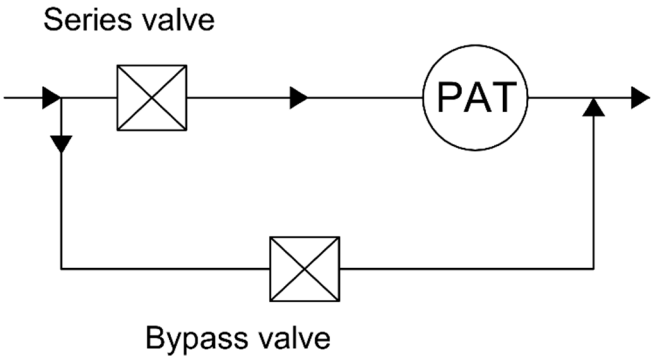

Figure 4. Hydropower plant with pump as turbine (PAT) and hydraulic regulation [17] (modified from [38]).

In Figure 3b, the daily trend of the head drop in the valve is given for the flow rate distribution of Figure 3a, as obtained in [17]. According to Figure 3, the daily average values of the discharge ($\overline{Q_F}$) and head loss within the PAT system ($\overline{\Delta H_{PAT}}$) are 4.35 L/s and 13 m, respectively. In addition, the minimum pressure head downstream of the valve to ensure a pressure of 10 m in the most critical node is 134 m. Finally, in Figure 3c, the daily trend of available power upstream of the valve is presented.

4. Drainage Discharge Pattern

A drainage network has been considered covering a part of the water supply area and conveying wastewater to a point close to the hydropower plant. According to the topography of the village, the direction of the wastewater flow produced by the inhabitants of the village has been predicted and a hypothetical drainage network has been overlaid on to the drinking water network, as shown in Figure 5.

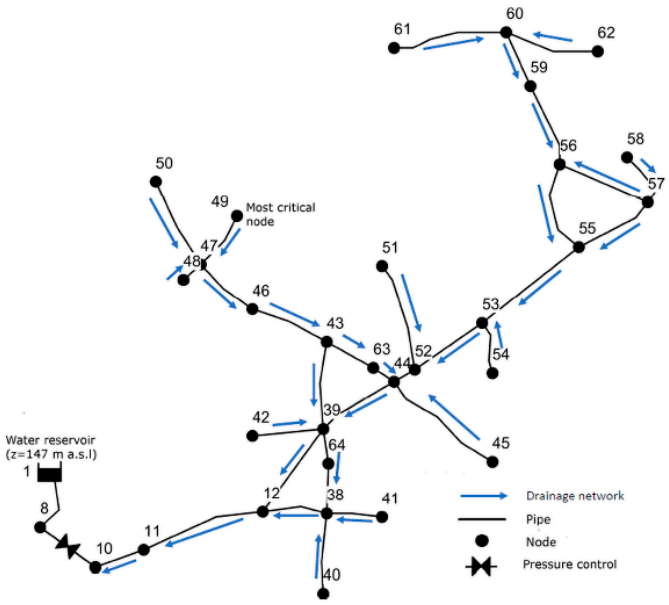

Figure 5. Layout of the drainage network.

The application of the MP&P here requires the calculation of a sewage discharge pattern. For such purposes, a response function had to be formulated, since freshwater input and the wastewater hydrograph are nonlinearly convoluted. As a reference inflow–outflow model, the Clark's model [39] has been chosen as an effective tool for simulating this kind of flow transformation. This model assumes the hydrologic response as a combination of two different functions, such as a translation and an attenuation function. In particular, the former function is reproduced by a linear channel, whereas the latter is represented by a single reservoir. Clarks Instantaneous Unit Hydrograph (CIUH) is shown in Equation (1).

$$\begin{cases} u(t) = \frac{1}{t_c}\left[1 - e^{-t/K}\right] & if\ t < t_c \\ u(t) = \frac{1}{t_c}\left[e^{-t/K}\left(e^{-t_c/K} - 1\right)\right] & if\ t > t_c \end{cases} \quad (1)$$

t_c is the time of concentration, namely, the travel time required by the head drop of the flow at the hydraulically most remote point of the catchment, to reach the storage tank; K is the storage coefficient, which accounts for the time delay between freshwater flow and the wastewater hydrograph. In the literature, many empirical expressions for K exist. In this paper, the formula proposed by [40] has been adopted:

$$K = t_c\, c \quad (2)$$

c is a coefficient accounting for the phenomenon of peak attenuation. This parameter has been set equal to 0.25, 0.5, and 0.75, thus around the value of 0.6, which is often used in literature [41].

Therefore, the sewage water hydrograph has been obtained by performing a convolution between the available fresh flow data and Clark Instantaneous Unit Hydrograph [40], as shown in Equation (3).

$$Q_S(t) = \int_0^t \varphi\, Q_F(\tau)\, u(t-\tau) d\tau \quad (3)$$

Q_S being the sewage discharge at a general time instant t; $d\tau$ is the convolution interval time, set at one minute; and φ the runoff coefficient, which does not take into account the rainfall.

Moreover, for the sake of generality, several wastewater hydrographs have also been obtained through the combination of different values of t_c, c, and φ. By varying φ, different sizes of flooding areas are considered. In particular, φ has been varied in a range between 0.1 and 0.8. According to Figure 6, φ_1, φ_2, and φ_3 represent three general runoff coefficient values in ascending order, which correspond to three increasing flooding areas.

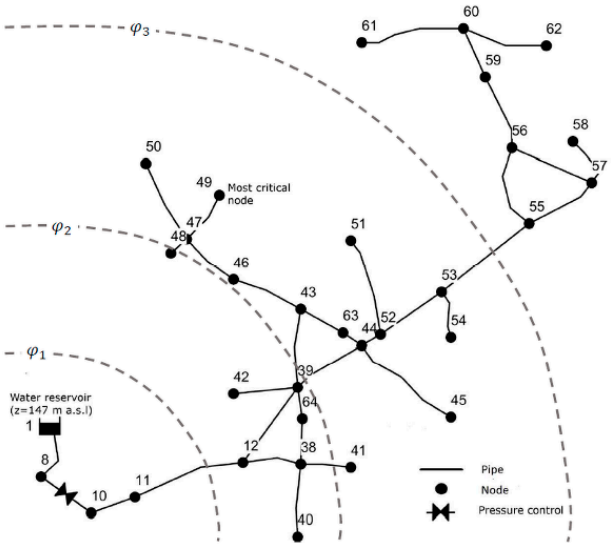

Figure 6. Different flooding areas in the network.

With regard to the time of concentration (t_c), the authors made an estimation by using the literature formula in Equation (4) [42], according to which the value for the specific case study resulted in around 1.5 h. Therefore, t_c has been varied between 1 and 2 h in this paper.

$$t_c = 1.7\, L_m^{0.6}\, S_m^{-0.3} \tag{4}$$

In Equation (4), L_m and S_m are the hydraulic length (in mile) and the slope (in feat/mile), both referring to the longest channel of the network.

As shown in Figure 7, by increasing t_c and c, the wastewater hydrograph diverges from the average fresh flow pattern. Furthermore, in Figure 7, a constant value of φ equal to 0.8 has been assumed.

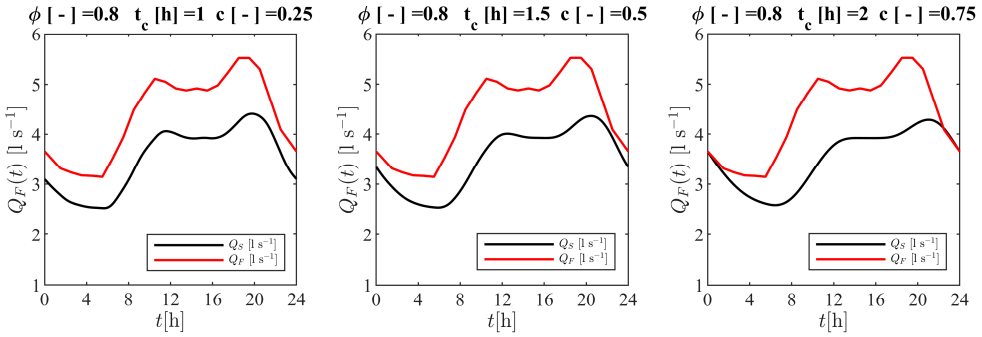

Figure 7. Average fresh flow pattern, and wastewater hydrographs for = 0.8 and different values of t_c and c.

The convergence of the drainage system into a point close to the hydropower plant (links 8–10) allows for the possibility of aligning a pump and PAT on a same shaft, where the freshwater and wastewater networks may be co-located. Compared to the turbo pumps used for water supply [21], the main difference here is represented by the time lag between the two curves: the peaks of the incoming discharge of the sewage systems are shifted with respect to the discharge pattern in the drinking water distribution system. This means that the peaks of the available power for turbining and the required power for pumping do not match. As an effect of that, when the maximum discharge is flowing through the sewage pipe, the available power may be not enough to pump out the full required flow rate. Therefore, a storage tank is required in order to compensate for this difference.

5. Pump and PAT Selection Strategy

A new strategy has been performed in order to select both the pump and PAT constituting the MP&P. This strategy allows for the selection of both machines, based on the maximum daily average fresh discharge ($\overline{Q_{F,max}}$) and the maximum daily average sewage discharge ($\overline{Q_{S,max}}$). A preliminary selection of the PAT can be done based on the maximum values of ΔH_{PAT} (see Section 3). The choice of the PAT can be not unique, because the rotational speed is not imposed. Once a PAT has been selected, its mechanical power, $P = P_{PAT} = P_P$, can be known from the performance curves of the machine. Thus, based on the values of discharge ($\overline{Q_{S,max}}$) and power (P), a pump can be selected from the pump manufacturer catalogues. Again, since the rotational speed is not known a priori, the choice of the pump is not unique, since different machines can exhibit similar performances at different rotational speeds. The real hydraulic characteristics of the system, as well as the rotational speed, depend on the mutual behavior of the two machines. Thus, the choice of the two machines should be validated, as explained hereafter. In this research, a large database of PAT curves was available, since this study is part of the REDAWN project (project EAPA 198/2016) of the European Union, which collected a large number of data on the reverse behavior of pumps. The selection involved three different PATs and five different pumps, and the coupling was validated for each of the possible combinations. In fact, only two different preliminary pump and PAT models have been chosen for the case study in question. Then, the PAT performance has been modified by varying the number of stages ($n_{st,PAT}$) from one to three, while for the pumps, five different impellers, differing by the diameter (D_P) ranging between 150 and 260 mm, have been tested hereafter. In particular, one centrifugal-multistage open-shaft sewage pump and one multistage centrifugal pump have been chosen.

Finally, for each possible coupling of a pump and PAT, the following equations have been solved:

$$\begin{cases} \left[a_{PAT}^N\left(\frac{\overline{Q_{F,max}}}{N}\right)^2 + b_{PAT}^N\left(\frac{\overline{Q_{F,max}}}{N}\right) + c_{PAT}^N\right]N^2\, n_{st,PAT} - \overline{\Delta H_{PAT,max}} = 0 \\ \left[a_P^N\left(\frac{\overline{Q_{S,max}}}{N}\right)^2 + b_P^N\left(\frac{\overline{Q_{S,max}}}{N}\right) + c_P^N\right]N^2 - \overline{H_{P,max}} = 0 \\ \alpha_P^N\left(\frac{\overline{Q_{S,max}}}{N}\right)^3 + \beta_P^N\left(\frac{\overline{Q_{S,max}}}{N}\right)^2 + \gamma_P^N\left(\frac{\overline{Q_{S,max}}}{N}\right) + \delta_P^N = \\ \left[\alpha_{PAT}^N\left(\frac{\overline{Q_{F,max}}}{N}\right)^3 + \beta_{PAT}^N\left(\frac{\overline{Q_{F,max}}}{N}\right)^2 + \gamma_{PAT}^N\left(\frac{\overline{Q_{F,max}}}{N}\right) + \delta_{PAT}^N\right]n_{st,PAT} \end{cases} \quad (5)$$

The three unknown variables N, $\overline{\Delta H_{PAT,max}}$, and $\overline{H_{P,max}}$ represent the rotational speed of both the pump and PAT, the daily average head dissipated by the PAT, and the daily average pressure head of the pump, respectively. The other parameters are a_{PAT}^N, b_{PAT}^N, c_{PAT}^N, α_{PAT}^N, β_{PAT}^N, γ_{PAT}^N, δ_{PAT}^N, a_P^N, b_P^N, c_P^N, α_P^N, β_P^N, γ_P^N, and δ_P^N, which represent the experimental regression coefficients of the head and the power curves of the PAT and pump. The experimental curves of the PAT for N = 1520 rpm and for the three stages, as well as the catalogue curves of the pump for different impeller diameters and N = 875 rpm, are shown in Figure 8. The curves of the PAT have been obtained by the experimental dataset of the REDAWN project (project EAPA 198/2016) of the European Union.

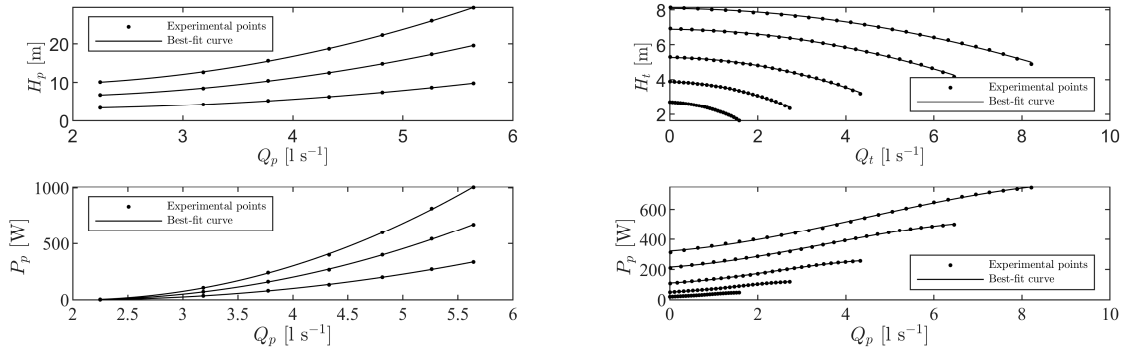

(**a**) (**b**)

Figure 8. Experimental curve of the pump as turbine (PAT) (**a**) for N = 1520 rpm and catalogue curve of the pump (**b**) for N = 875 rpm.

Finally, $\overline{Q_{S,max}}$ is the maximum daily average sewage discharge, and this has been set equal to $\varphi\ \overline{Q_{F,max}}$. $\overline{Q_{F,max}}$ is the maximum daily average fresh discharge, and was equal to 5.5 L/s. Furthermore, the runoff coefficient φ has been varied in a range between 0.1 and 0.8.

Figure 9 shows the behavior of the system when $n_{st,PAT} = 1$, $D_P = 260$ mm, and $\varphi = 0.2$ as an example. The top plot of Figure 9 shows the power versus the rotational speed when the discharge is assigned. In particular, the blue line represents the power produced by the PAT when the turbined discharge is $\overline{Q_{F,max}} = 5.5$ L/s—the left-hand side of the third equation of the set (5)—while the red line shows the power absorbed by the pump when the pumped flow rate is $\overline{Q_{S,max}} = \varphi\ \overline{Q_{F,max}}$—the left-hand side of the third equation of the set (5). The intersection point of the two curves represents the operating rotational speed of the turbocharger. The bottom plot of Figure 9 shows the head jump in the PAT, $\overline{\Delta H_{PAT,max}}$, and the head of the pump, $\overline{H_{P,max}}$, versus the rotational speed. For the operating speed, the head jump of the turbine is lower than the maximum allowed value (13.5 m), while the pumping head is $\overline{H_{P,max}} = 6.69$ m.

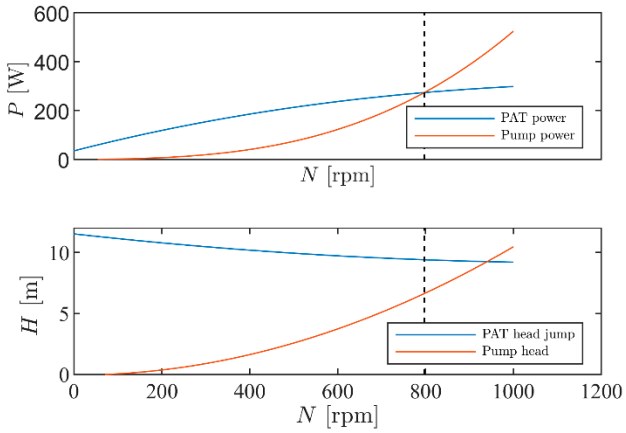

Figure 9. Power and head curve versus rotational speed for the PAT and the pump, respectively, when $n_{st,PAT} = 1$, $D_P = 260$ mm, and $\varphi = 0.2$.

Figure 10 shows the behavior of the turbocharger for the same conditions of Figure 9. The four curves have been calculated for N = 797 rpm, which resulted from the calculation. The head of the PAT is showed in the left-bottom plot. For the sake of illustration, let the turbined discharge be 5.5 L/s: the operating point lies below the red line, which represents the maximum allowed head jump. The output power of the PAT and the input power of the pump are equal to 273 W, while the pumped discharge is equal to 1.1 L/s, as shown by the comparison of the two top plots. The pumping head is instead shown in the right-bottom plot.

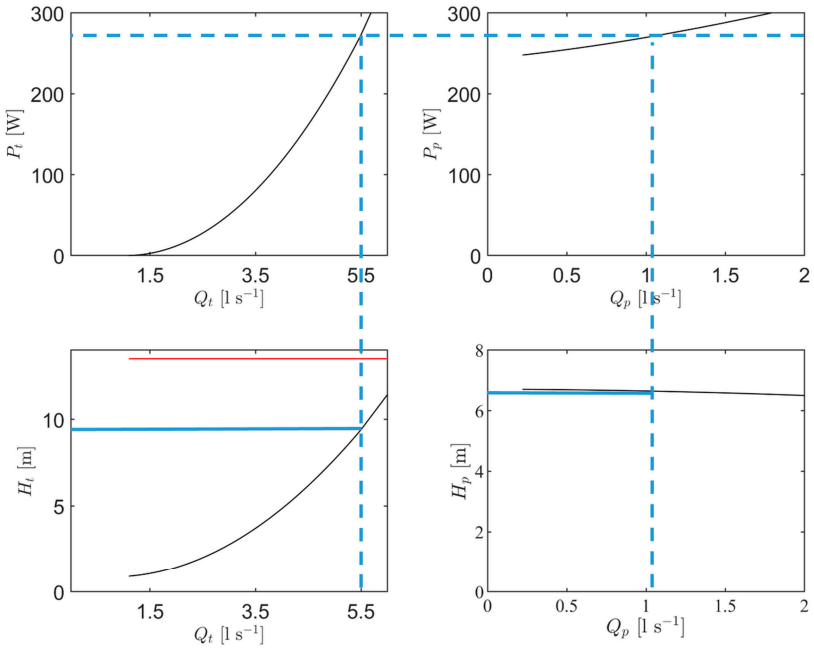

Figure 10. Operation of the plant for N = 797 rpm, $n_{st,PAT} = 1$, $D_P = 260$ mm, and $\varphi = 0.2$. (The red line is the maximum allowed head jump within the PAT, which is 13.5 m).

For each combination ($n_{st,PAT}$, D_P), and thus for each possible coupling of pump–PAT, several operating conditions have been obtained. The values of $\overline{\Delta H_{PAT,max}}$ and $\overline{H_{P,max}}$ resulting from the resolution of the system (5) will be employed to select the most advantageous combination of pump and PAT for the MP&P plant, as further will be explained. For the sake of illustration, Table 1 shows the results obtained for φ equal to 0.2.

Table 1. Main figures of preliminary design for $\varphi = 0.2$.

$n_{st,PAT}$ (-)	D_P (m)	$\overline{H_{P,max}}$ (m)	$\overline{\Delta H_{PAT,max}}$ (m)
1	0.15	3.79	9.24
1	0.18	5.21	9.28
1	0.21	5.47	9.38
1	0.24	6.15	9.44
1	0.26	6.69	9.48
2	0.15	6.32	18.64
2	0.18	8.86	18.50
2	0.21	9.46	18.46
2	0.24	10.70	18.48
2	0.26	11.65	18.51
3	0.15	8.28	28.64
3	0.18	11.73	28.18
3	0.21	12.70	27.80
3	0.24	14.42	27.72
3	0.26	15.74	27.69

According to Table 1, the number of stages of the PAT equal to two and three will not be considered any longer, since the corresponding value of $\overline{\Delta H_{PAT,max}}$ exceeds 13.5 m, which represents the maximum value of head that can be dissipated by the PAT, according to Figure 3b. Thus, only the one-stage PAT will be further considered. Furthermore, among all the pump diameters, D_P as 0.26 m has been chosen, since it ensures greater values of both pressure ($\overline{H_{P,max}}$) and dissipated head $\overline{\Delta H_{PAT,max}}$ for an assigned number of stages, according to Table 1. Since values of $\overline{H_{P,max}}$ and $\overline{\Delta H_{PAT,max}}$ in Table 1 referred to the

maximum daily average discharge in the network, the operation of both pump and PAT will be further verified in Section 6 considering the instantaneous values of discharge across the day.

This pump selection strategy has been useful to perform a preliminary geometric selection of both the pump and PAT constituting the turbo pump. The behavior of the MP&P should be otherwise simulated as many times as the number of all possible machines, which may suit the operating conditions.

6. Simulation of the Behavior of the MP&P

Before having carried on with the simulation of the mixed PAT–pump turbocharger behavior, some variables (previously presented in Section 2) have been set. In particular:

1) Q_F and Q_S have been set according to Figures 3a and 7, respectively;
2) H_1^u is equal to the hydraulic head in the node upstream of the power plant inlet, which is estimated by the hydraulic simulator Epanet [36].
3) H_2^d is the required head to pump the water from the wet tank to the inlet of the treatment plant. It depends on the water level within the wet tank, the elevation of the treatment plant, and the head losses in the pipeline. It is a design parameter, and the machine selection procedure should enable the accomplishment of this. In this case, since no real-world information is available about the sewage system, it has been chosen as a function of the pump head resulting from the selection procedure, while the head losses in the pipeline have been neglected. Therefore, H_2^d has been calculated as:

$$H_2^d = \frac{W_1}{\Sigma} + \overline{H_{P.min}}. \tag{6}$$

W_1 and Σ are the volume and cross-sectional area of the water tank, set equal to 1.5 m^3 and 1 m^2, respectively.

Then, in order to perform the simulation of the MP&P behavior, a mathematical system of five equations has been solved.

$$\begin{cases} \alpha_P^N\left(\frac{Q_P}{N{D_P}^3}\right)^3 + \beta_P^N\left(\frac{Q_P}{N\,{D_P}^3}\right)^2 + \gamma_P^N\left(\frac{Q_P}{N\,{D_P}^3}\right) + \delta_P^N = \\ \alpha_{PAT}^N\left(\frac{Q_F}{N\,{D_{PAT}}^3}\right)^3 + \beta_{PAT}^N\left(\frac{Q_F}{N\,{D_{PAT}}^3}\right)^2 + \gamma_{PAT}^N\left(\frac{Q_F}{N\,{D_{PAT}}^3}\right) + \delta_{PAT}^N \\ H_1^u - H_1^d - \left[a_{PAT}^N\left(\frac{Q_F}{N\,{D_{PAT}}^3}\right)^2 + b_{PAT}^N\left(\frac{Q_F}{N\,{D_{PAT}}^3}\right) + c_{PAT}^N\right]N^2{D_{PAT}}^2 = 0 \\ H_2^d - H_2^u - \left[a_P^N\left(\frac{Q_P}{N\,{D_P}^3}\right)^2 + b_P^N\left(\frac{Q_P}{N\,{D_P}^3}\right) + c_P^N\right]N^2{D_P}^2 = 0 \\ Q_S - Q_P - \Sigma\frac{dH_2^u}{dt} + \frac{Q_P}{\left(H_2^u+1\right)^{20}} = 0 \end{cases} \tag{7}$$

The solution of this set of equation allows predicting the complete behavior of the system. Indeed, the four unknown variables are N, Q_P, H_2^u, and H_1^d. According to the system (7), the first equation states that the power at the shaft is the same for both the PAT and pump; the second equation expresses the negative head drop in the PAT (namely, ΔH_{PAT} in Figure 1) as the difference between the head available at the power plant inlet and outlet; the third equation states the positive head drop in the pump as the difference between the hydraulic head at the pumping station outlet and inlet; finally, the latter is the continuity equation of the wet tank, which is characterized by its cross-sectional area Σ. In particular, in the latter equation, the last term represents the bypass discharge (Q_{BP}). In system (7), affinity laws have been used to simulate the behavior of the machines under variable speed [43].

Concerning the resolution of the mathematical system (7), the differential equation was solved using the finite differences method; in particular, a first-order backward numerical scheme has been used. In addition, a time step equal to one minute has been assumed, and a six-day simulation was performed. Hereafter, the results will refer to the last 24 h of the whole simulation, in order to omit any

dependency on the initial level in the wet tank from the results. Furthermore, the mathematical system (7) has been solved by applying the Newton Raphson method [44].

For the sake of generality, results that are presented hereafter correspond to only one configuration, i.e., $\varphi = 0.7$, $t_c = 1$ h, and $c = 0.25$. For this configuration, the pattern of fresh and sewage discharge is shown in Figure 11.

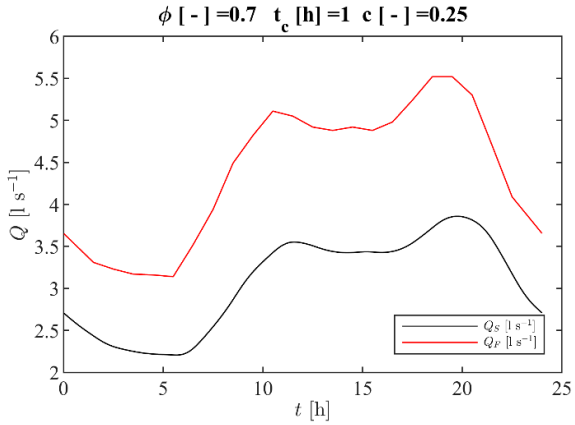

Figure 11. Time series of fresh and sewage discharge, for $\varphi = 0.7$, $t_c = 1$ h, and $c = 0.25$.

Figure 12 shows the trend of unknown variables as functions of the time. According to Figure 12, the water level in the tank (H_2^u) and pumped wastewater discharge (Q_P) are strictly related: a reduction of the water level is due to an increase in pumped discharge, and vice versa. Note that the zero values of H_2^u do not correspond to the empty wet well, but just to the minimum level in order to avoid cavitation in the pumping system. The cavitation problem is indeed overcome by the employment of the bypass, which avoids the emptying of the tank when the pumped flow is too high. Furthermore, as regards the head downstream of the hydropower plant, namely, H_1^d, it has been ensured to be always greater than the minimum allowed value, i.e., 134 m, which is the smallest value of the downstream head over the day that is required to guarantee a minimum pressure of 10 m in the most critical node of the network (node 49). This result means that with the MP&P plant, only a part of the available head is enough to pump the wastewater to the treatment plant. Note that the pressure downstream of the PAT is always enough to avoid any cavitation problem. Of course, a higher head loss is produced when the discharge flowing into the PAT is higher. On the contrary, all of the available head (and thus the available power) is used when a PAT and a generator are installed to produce electricity.

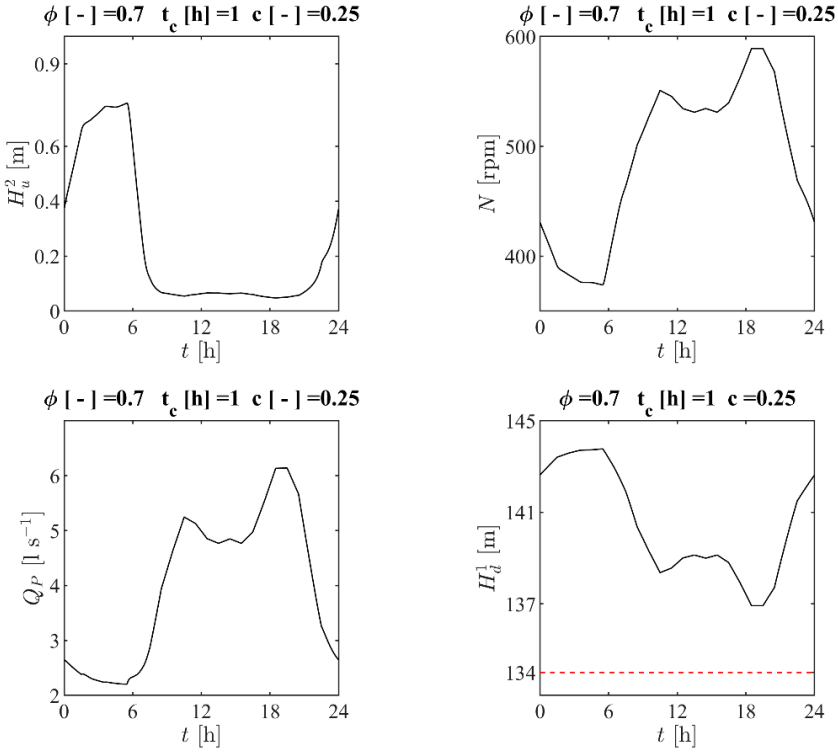

Figure 12. Time series of unknown variables of system (7).

In the next section, an economic analysis of the two situations is presented to compare the two options for the real case. Finally, according to Figure 12, the trend of rotational speed (N) follows the trend of pumped wastewater discharge (Q_P).

7. Economic Comparison

In order to assess the economic benefit of the mixed PAT–pump turbocharger, an economic comparison has been performed with a conventional wastewater pumping system, working in ON/OFF mode. The economic comparison has been performed by assessing the net present value (NPV) of the investment in both scenarios, for each configuration (t_c, c, φ). Since the number of valves and bypass is the same in both the scenarios—as shown in Figure 1—the corresponding costs will be therefore neglected in the economic computation, as well as the cost of the hydraulic pump and PAT. As regards the MP&P scenario, the NPV can be therefore expressed as:

$$NPV_1 = \sum_{y=0}^{Y} \frac{C_{1,y}^{in} - C_{1,y}^{out}}{(1+r)^y} = -C_{1,y=0}^{out} = -C_{1,W}^{tank}. \quad (8)$$

In Equation (8), Y is the number of y years, C_y^{in} and C_y^{out} are the cash inflow and outflow, respectively, at the $y-th$ year, and r represents the discount rate, which is set equal to 5%. Moreover, $C_{1,y}^{in}$ is equal to zero since the energy recovered by the PAT does not represent a gain; it is being used to supply the pump. Concerning the cash outflow in the mixed PAT–pump turbocharger scenario, namely $C_{1,y}^{out}$, it consists of the purchasing cost faced at the first year, made by only the cost of the water tank, $C_{1,W}^{tank}$. With regard to the construction cost of the holding tank, this has not been accounted in the cash outflow, since it has been assumed that such a tank already existed previously, in order to contain the hydrovalve.

In order to evaluate $C_{1,W}^{tank}$, a price list [45] has been employed. In particular, since the tank is characterized by a volume of 1.5 m^3 and a cross-sectional area equal to 1 m^2, the cost of a prefabricated tank having a dimension of (150 cm × 150 cm × 90 cm) has been adopted. In conclusion, due to the

neglected terms, the NPV_1 is represented by the investment cost of the water tank, which is equal to approximately 300 €. As regards the conventional system, the NPV has been calculated as:

$$NPV_2 = \sum_{y=0}^{Y} \frac{C_{2,y}^{in} - C_{2,y}^{out}}{(1+r)^y} = -C_{2,y=0}^{out} + \sum_{y=1}^{Y} \frac{C_{2,y}^{E\_PAT} - C_{2,y}^{E\_pump}}{(1+r)^y}. \quad (9)$$

According to Equation (9), $C_{2,y}^{E\_PAT}$ is the cost associated with the recovered energy, whereas $C_{2,y}^{E\_pump}$ is the cost of the energy spent to pump the wastewater discharge. Finally,$C_{2,y=0}^{out}$ represents the purchasing cost faced at the first year, which is expressed as Equation (A1) (see Appendix A).

Conversely to the mixed PAT–pump turbocharger, in which the whole energy produced by the PAT is employed to pump the wastewater, in the conventional scheme, both the costs associated to recovered and absorbed energy have been taken into account to evaluate the NPV. For each configuration (c, t_c, φ), the cost of the spent energy has been calculated as:

$$C_2^{E\_pump} = \int_{day} \frac{\gamma\, Q_S\, \overline{H_P}\, c_u}{\eta_{2,M}\, \eta_{2,P}}\, dt. \quad (10)$$

In Equation (10), dt is equal to one minute, and $\overline{H_P}$ represents the daily average pressure head, calculated as:

$$\overline{H_P} = H_2^d - \overline{H_2^u}. \quad (11)$$

$\overline{H_2^u}$ being the daily average water level in the tank. In addition, according to Equation (10), $\eta_{2,M}$ is the motor efficiency, which has been set equal to 0.8, and c_u represents the energy cost distribution, as shown in Figure 13.

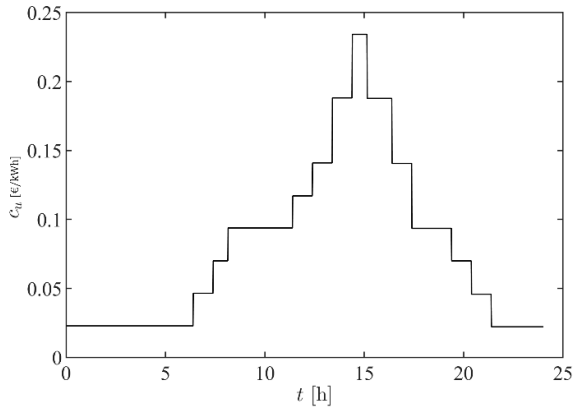

Figure 13. Energy cost distribution over time.

Finally, as regards $\eta_{2,P}$, it represents the hydraulic pump efficiency at the best efficiency point (BEP) condition, equal to 0.6. Thus, for each configuration (c, t_c, φ), a different pump is assumed, having the same efficiency as the BEP condition of the pump employed in MP&P. Finally:

$$C_2^{E\_PAT} = \int_{day} P_{2,PAT}\, c_u \eta_{2,GEN}\, dt. \quad (12)$$

$P_{2,PAT}$ being the power produced by the PAT and $\eta_{2,GEN}$ the efficiency of the generator, which were both calculated in [17].

8. Discussion

The NPV has been calculated by considering time periods equal to 5, 10, and 20 years. The main figures of the comparison are shown in Table 2, in which the difference between NPV_1 and NPV_2 at time periods of 5, 10, and 20 years has been divided for the average pumped power ($\overline{P_{hyd}}$), resulting in ΔNPV_5, ΔNPV_{10}, and ΔNPV_{20}, respectively. This amount represents the economic convenience of the mixed PAT–pump turbocharger over the conventional system.

Table 2. Main figures of the economic comparison.

t_c (h)	c (-)	φ (-)	$\overline{H_P}$ (m)	$\overline{P_{hyd}}$ (W)	ΔNPV_5 (€/kW)	ΔNPV_{10} (€/kW)	ΔNPV_{20} (€/kW)
1.00	0.25	0.20	2.17	67.84	23,825	15,922	4878
1.00	0.25	0.50	1.63	73.01	24,180	18,435	10,407
1.00	0.25	0.80	1.07	66.44	27,257	21,484	13,417
1.00	0.50	0.20	2.17	67.86	23,809	15,900	4846
1.00	0.50	0.50	1.63	73.00	24,160	18,397	10,345
1.00	0.50	0.80	1.07	66.37	27,248	21,438	13,319
1.00	0.75	0.20	2.17	67.88	23,789	15,873	4811
1.00	0.75	0.50	1.63	73.00	24,138	18,356	10,276
1.00	0.75	0.80	1.05	66.29	27,239	21,388	13,211
1.50	0.25	0.20	2.17	67.86	23,802	15,889	4831
1.50	0.25	0.50	1.63	73.00	24,150	18,379	10,314
1.50	0.25	0.80	1.06	66.33	27,244	21,414	13,267
1.50	0.50	0.20	2.16	67.90	23,770	15,848	4777
1.50	0.50	0.50	1.62	72.99	24,116	18,314	10,206
1.50	0.50	0.80	1.04	66.20	27,230	21,336	13,100
1.50	0.75	0.20	2.16	67.96	23,731	15,801	4718
1.50	0.75	0.50	1.60	72.97	24,078	18,242	10,088
1.50	0.75	0.80	0.99	66.09	27,208	21,251	12,927
2.00	0.25	0.20	2.16	67.90	23,772	15,849	4778
2.00	0.25	0.50	1.63	72.99	24,117	18,316	10,208
2.00	0.25	0.80	1.04	66.19	27,232	21,337	13,100
2.00	0.50	0.20	2.16	67.97	23,721	15,787	4701
2.00	0.50	0.50	1.60	72.97	24,067	18,221	10,051
2.00	0.50	0.80	0.97	66.04	27,204	21,224	12,868
2.00	0.75	0.20	2.16	68.05	23,665	15,720	4616
2.00	0.75	0.50	1.56	72.95	24,013	18,119	9883
2.00	0.75	0.80	0.91	65.93	27,162	21,103	12,635

Firstly, it is worth highlighting that the figures in Table 2 are small due to the small size of the case study network (indeed, the mean flow rate from the reservoir is only 4.35 L/s). Nevertheless, the obtained results are meaningful to investigate the performance of the MP&P plant. Furthermore, according to Table 2, MP&P is shown to be the most economically advantageous scenario, since the values of ΔNPV are positive. Moreover, this advantage over the conventional approach reduces with the increasing time periods. In the conventional system, the production of energy amortizes the investment costs over time. As shown in Table 2, by increasing φ, the advantage of MP&P increases, since in the conventional scheme, the increase of pumped wastewater is not compensated by the reduction of pressure head. This result is further shown in Figure 14.

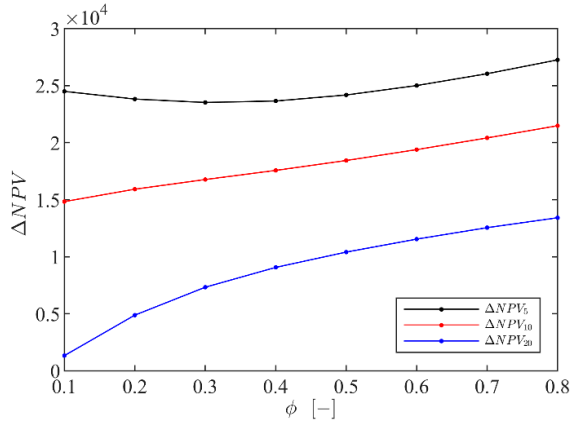

Figure 14. Difference of net present value (NPV) between both the scenarios against the runoff coefficient (φ), for different time periods (5, 10, and 20 years).

As shown in Figure 15, by increasing φ from 0.2 to 0.5, and thus increasing the sewage water by 150%, the pressure head reduces by only 24%; thus, $C_2^{E\_pump}$ increases. As a result, the MP&P results become more economically attractive than the conventional scheme. By increasing φ from 0.2 to 0.8, such convenience amounts to 14% after a time period of five years. Furthermore, the convenience of MP&P increases to 34% and 175% up to time periods equal to 10 and 20 years, respectively.

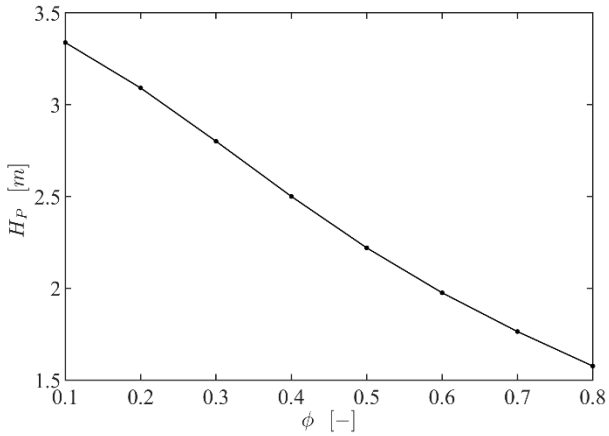

Figure 15. Daily averaged pressure head ($\overline{H_P}$) against runoff coefficient (φ).

On the other hand, according to Table 2, the NPV seems to be not very sensitive to the variation of c and t_c.

Definitively, the MP&P system can be certainly preferred over the conventional system up to a time period of 20 years, i.e., the useful life of the plant, beyond which the cash inflow due to the production of energy overcomes the initial cash outflow.

In the MP&P plant, the absence of electric devices significantly reduces the need for maintenance and repair works. Nevertheless, as the maintenance costs are not easily assessable due to the scarcity of data in the literature, in the evaluation of ΔNPV, such costs have been considered the same in both the plants, in order to avoid pushing the comparison in favor of the MP&P plant.

Despite the advantages of the mixed PAT–pump turbocharger highlighted here, it is worth noting that the feasibility of the plant is restricted to cases in which the wastewater pumping station can be aligned to the point of excess pressure of the water network. On the other hand, this kind of configuration is not uncommon, since a point of excess pressure lies in a low ground-level area, hence the need for a pumping station to convey wastewater.

9. Conclusions

In this paper, a new strategy to increase the energy efficiency of a water system is analyzed. This strategy comprises a plant consisting of a pump and PAT mounted on the same shaft: the PAT is employed to convert the excess head from a fresh flow rate to energy, in order to supply a pump conveying a wastewater stream into a treatment plant. This configuration arises whenever it is possible to realize the co-location of a point of excess pressure dissipation with a wastewater pumping station. Therefore, the feasibility of the plant depends on the topography of the network.

To facilitate the design of the plant, a preliminary method to select the appropriate machines has been developed, based on the maximum daily averaged values of fresh and wastewater discharge. These new equations allow for the selection of the pump and of the PAT, once two among the four average hydraulic characteristics of the wastewater and freshwater stream (namely the discharge and the head jump of the two flows) are given. According to the results of this strategy, a centrifugal pump with a diameter equal to 260 mm has been selected, whereas the resulting PAT has been the one stage centrifugal pump, with a diameter equal to 142 mm.

Hereafter, the behavior of the mixed PAT–pump turbocharger has been simulated by means of a mathematical system consisting of four equations. The resolution of this system has allowed for the determination of the values of the shaft rotational speed, as well as the wastewater pumped discharge, the water level in the wet tank, and the value of pressure downstream of the MP&P plant, at 1-min intervals. Moreover, for the sake of generality, the behavior of the plant has been investigated for several wastewater hydrographs.

Furthermore, in order to assess the benefits of the plant, an economic comparison with a conventional wastewater pumping system working in ON/OFF mode has been performed. The comparison is based on the evaluation of the net present value of the investment in both scenarios, which was calculated for different time periods and for several wastewater hydrographs. The comparison has shown the advantages of the MP&P plant, whose investment consists of only the purchase of hydraulic machines, pipes, valves, a wet tank, and a holding tank. Moreover, further costs related to the wastewater pumping have not been taken into account, as the pump was supplied only by energy produced by the PAT. Conversely, the conventional scheme is characterized by additional costs related to the motor and the generator, as well as to the energy spent for pumping. Definitively, the comparison has shown that the mixed PAT–pump turbocharger represents the most economically viable configuration, at least until the useful life of the plant is reached.

Despite the promising results, the plant presents some limitations. First of all, it may be possible that the point of pressure dissipation is not close enough to the pumping station; thus, the PAT and pump could not be practically coupled on the same shaft. Furthermore, due to the small available power, this plant may be not employed in a mixed storm–wastewater sewage, unless an auxiliary pump is chosen. Moreover, a further limitation may be consequent to the lack of PAT performance curves: therefore, mathematical systems (5) and (7) may not be solvable. Finally, this plant should require sanitary measures in order to avoid the contamination of freshwater by the sewage.

In this research, storm water has not been taken into account. Nevertheless, the plant may be employed to empty a wet retention basin in a storm water sewage.

Author Contributions: Conceptualization, M.C.M., A.C., O.F. and A.M.N.; methodology, M.C.M., A.C., O.F. and A.M.N.; software, M.C.M., O.F.; validation M.C.M., A.C., O.F. and A.M.N.; formal analysis, M.C.M., A.C., O.F. and A.M.N.; investigation, M.C.M., A.C., O.F. and A.M.N.; resources, M.C.M., A.C., O.F. and A.M.N.; data curation, M.C.M., A.C., O.F. and A.M.N.; writing—original draft preparation M.C.M., A.C., O.F. and A.M.N.; writing—review and editing, M.C.M., A.C., O.F. and A.M.N.; visualization, M.C.M., A.C., O.F. and A.M.N.; supervision, M.C.M., A.C., O.F. and A.M.N.; project administration, M.C.M., A.C., O.F. and A.M.N.; funding acquisition, M.C.M., A.C., O.F. and A.M.N. All authors have read and agreed to the published version of the manuscript.

Funding: This paper was partly funded by the ERDF (European Regional Development Fund) Interreg Atlantic Area Programme 2014–2020, through the REDAWN (Reduction Energy Dependency in Atlantic area Water Networks) project EAPA 198/2016.

Conflicts of Interest: The authors declare no conflict of interest.

Appendix A

In the conventional system, the purchasing cost faced at the first year can be expressed as:

$$C_{2,y=0}^{out} = C_{2,MOT} + C_{2,GEN} + C_{2,W}^{tank}. \quad \text{(A1)}$$

Unlike the mixed PAT–pump turbocharger scenario, Equation (A1) takes into account the costs of the motor and generator. $C_{2,MOT}$ is the cost of the pump motor, and $C_{2,GEN}$ is the cost of the PAT generator. Finally, $C_{2,W}^{tank}$ is the cost of the water tank. In order to evaluate $C_{2,MOT}$, a commercial catalogue by [46] has been consulted, and a cost function has been obtained as polynomial best fit curve, as shown in Figure A1.

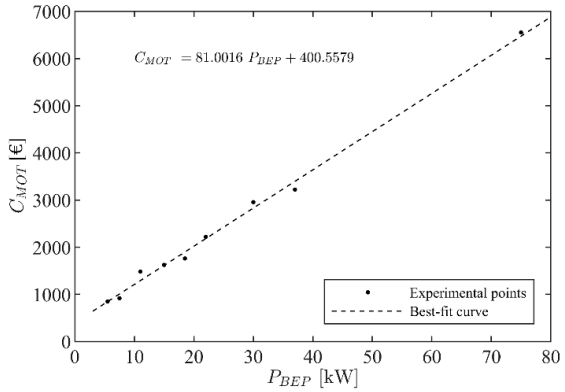

Figure A1. Commercial costs and polynomial best fit curve.

With regard to the PAT, a centrifugal multistage end-suction pump HMU50-2/2 [46] has been chosen as the reference machine, since it has been already designed and optimized in [17] in order to maximize the energy produced in this network. Therefore, in order to evaluate $C_{2,GEN}$, a generator cost function [47] has been employed, as shown in Equation (A2).

$$C_{gen}[€] = 60.19\ P[\text{kW}] + 163.15 \quad \text{(A2)}$$

where P is the power produced at the best efficiency point (BEP), expressed in kW.

Equation (A2) refers to a generator characterized by three pairs of poles [47]. In fact, as shown in [17], the optimal configuration is characterized by a PAT working at a rotating speed equal to 1025 rpm. Furthermore, in order to evaluate the water tank cost, $C_{2,W}^{tank}$, the computation of the preliminary tank volume is required. The volume has been calculated by Equation (A3) [15]:

$$W_2 = \max_{c,t_c,\varphi}\left(\frac{900\ Q_{MAX}}{n_{av}}\right) \quad \text{(A3)}$$

where n_{av} is the number of pump starts per hour, set equal to eight, as suggested by the technical catalogue, and Q_{MAX} is the maximum discharge, which is calculated as:

$$Q_{MAX} = \alpha\ Q_{S,max}^{c,t_c,\varphi} \quad \text{(A4)}$$

where $Q_{S,max}^{c,t_c,\varphi}$ is the maximum wastewater discharge for an established combination (c, t_c, φ) and α is a safety factor, which has been set equal to two. This safety factor accounts for the random variation around the daily average peak value $Q_{S,max}^{c,t_c,\varphi}$. The volume W_2 resulted in a volume of 0.5 m^3 and the corresponding price, $C_{2,W}^{tank}$, has been obtained from commercial price lists [45], as in the MP&P scenario.

References

1. Xue, X.; Hawkins, T.; Schoen, M.; Garland, J.; Ashbolt, N. Comparing the Life Cycle Energy Consumption, Global Warming and Eutrophication Potentials of Several Water and Waste Service Options. *Water* **2016**, *8*, 154. [CrossRef]
2. Abbott, M.; Cohen, B. Productivity and efficiency in the water industry. *Util. Policy* **2009**, *17*, 233–244. [CrossRef]
3. Olsson, G. *Water and Energy: Threats and Opportunities*, 2nd ed.; IWA publishing: London, UK, 2015.
4. Colombo, A.F.; Karney, B.W. Energy and Costs of Leaky Pipes: Toward Comprehensive Picture. *J. Water Resour. Plan. Manag.* **2002**, *128*, 441–450. [CrossRef]
5. Ramos, H.M.; Vieira, F.; Covas, D.I.C. Energy efficiency in a water supply system: Energy consumption and CO2 emission. *Water Sci. Eng.* **2010**, *3*, 331–340.
6. Ainger, C.; Butler, D.; Caffor, I.; Crawford-brown, D.; Helm, D.; Stephenson, T. *A Low Carbon Water Industry in 2050*; EA Report: SC070010/R3; Environment Agency: Bristol, UK, December 2009.
7. Zema, D.A.; Nicotra, A.; Tamburino, V.; Zimbone, S.M. A simple method to evaluate the technical and economic feasibility of micro hydro power plants in existing irrigation systems. *Renew. Energy* **2016**, *85*, 498–506. [CrossRef]
8. Hadian, S.; Madani, K. A system of systems approach to energy sustainability assessment: Are all renewables really green? *Ecol. Indic.* **2015**, *52*, 194–206. [CrossRef]
9. Cabrera, E.; Pardo, M.A.; Cobacho, R.; Cabrera, E.J. Energy Audit of Water Networks. *J. Water Resour. Plan. Manag.* **2010**, *136*, 669–677. [CrossRef]
10. Castro-Gama, M.; Pan, Q.; Lanfranchi, E.A.; Jonoski, A.; Solomatine, D.P. *Pump Scheduling for a Large Water Distribution Network*; Elsevier: Milan, Italy, 2017; pp. 436–443.
11. Sperlich, A.; Pfeiffer, D.; Burgschweiger, J.; Campbell, E.; Beck, M.; Gnirss, R.; Ernst, M. Energy efficient operation of variable speed submersible pumps: Simulation of a ground water well field. *Water* **2018**, *10*, 1255. [CrossRef]
12. Giacomello, C.; Kapelan, Z.S.; Nicolini, M. Fast Hybrid Optimization Method for Effective Pump Scheduling. *Water Resour. Plan. Manag.* **2013**, *139*, 175–183. [CrossRef]
13. Ostojin, S.; Mounce, S.; Boxall, J.B. An artificial intelligence approach for optimizing pumping in sewer systems. *J. Hydroinform.* **2011**, *13*, 295–306. [CrossRef]
14. Chabal, L.; Stanko, S. Sewerage Pumping Station Optimization Under Real Conditions. *Geosci. Eng.* **2015**, *60*, 19–28. [CrossRef]
15. Fecarotta, O.; Carravetta, A.; Morani, M.C.; Padulano, R. Optimal Pump Scheduling for Urban Drainage under Variable Flow Conditions. *Resources* **2018**, *7*, 73. [CrossRef]
16. Fecarotta, O.; Martino, R.; Morani, M.C. Wastewater pump control under mechanical wear. *Water* **2019**, *11*, 1210. [CrossRef]
17. Morani, M.C.; Carravetta, A.; Del Giudice, G.; McNabola, A.; Fecarotta, O. A Comparison of Energy Recovery by PATs against Direct Variable Speed Pumping in Water Distribution Networks. *Fluids* **2018**, *3*, 41. [CrossRef]
18. Carravetta, A.; Fecarotta, O.; Ramos, H.M. A new low-cost installation scheme of PATs for pico-hydropower to recover energy in residential areas. *Renew. Energy* **2018**, *125*, 1003–1014. [CrossRef]
19. Arriaga, M. Pump as turbine—A pico-hydro alternative in Lao People's Democratic Republic. *Renew. Energy* **2010**, *35*, 1109–1115. [CrossRef]
20. Giugni, M.; Fontana, N.; Ranucci, A. Optimal Location of PRVs and Turbines in Water Distribution Systems. *J. Water Resour. Plan. Manag.* **2014**, *140*, 6014004. [CrossRef]
21. Carravetta, A.; Antipodi, L.; Golia, U.; Fecarotta, O. Energy saving in a water supply network by coupling a pump and a Pump As Turbine (PAT) in a turbopump. *Water* **2017**, *9*, 62. [CrossRef]
22. Fecarotta, O.; McNabola, A. Optimal Location of Pump as Turbines (PATs) in Water Distribution Networks to Recover Energy and Reduce Leakage. *Water Resour. Manag.* **2017**, *31*, 5043–5059. [CrossRef]
23. Campisano, A.; Modica, C.; Vetrano, L. Calibration of Proportional Controllers for the RTC of Pressures to Reduce Leakage in Water Distribution Networks. *J. Water Resour. Plan. Manag.* **2012**, *138*, 377–384. [CrossRef]
24. Stokes, J.R.; Horvath, A.; Sturm, R. Water loss control using pressure management: Life-cycle energy and air emission effects. *Environ. Sci. Technol.* **2013**, *47*, 10771–10780. [CrossRef] [PubMed]

25. Schwaller, J.; van Zyl, J.E. Modeling the Pressure-Leakage Response of Water Distribution Systems Based on Individual Leak Behavior. *J. Hydraul. Eng.* **2014**, *141*, 04014089. [CrossRef]
26. Pérez-Sánchez, M.; Sánchez-Romero, F.J.; Ramos, H.M.; López-Jiménez, P.A. Energy recovery in existing water networks: Towards greater sustainability. *Water* **2017**, *9*, 97. [CrossRef]
27. Ramos, H.M.; Mello, M.; De, P.K. Clean power in water supply systems as a sustainable solution: From planning to practical implementation. *Water Sci. Technol. Water Supply* **2010**, *10*, 39. [CrossRef]
28. McNabola, A.; Coughlan, P.; Corcoran, L.; Power, C.; Williams, A.P.; Harris, I.; Gallagher, J.; Styles, D. Energy recovery in the water industry using micro-hydropower: An opportunity to improve sustainability. *Water Policy* **2014**, *16*, 168–183. [CrossRef]
29. Gallagher, J.; Styles, D.; McNabola, A.; Williams, A.P.P. Life cycle environmental balance and greenhouse gas mitigation potential of micro-hydropower energy recovery in the water industry. *J. Clean. Prod.* **2015**, *99*, 152–159. [CrossRef]
30. Fecarotta, O.; Ramos, H.M.; Derakhshan, S.; Del Giudice, G.; Carravetta, A. Fine Tuning a PAT Hydropower Plant in a Water Supply Network to Improve System Effectiveness. *J. Water Resour. Plan. Manag.* **2018**, *144*, 04018038. [CrossRef]
31. Carravetta, A.; Derakhshan Houreh, S.; Ramos, H.M. *Pumps as Turbines: Fundamentals and Applications*; Springer: Cham, Switzerland, 2018; pp. 3–26. ISBN 978-3-319-67506-0.
32. Derakhshan, S.; Nourbakhsh, A. Experimental study of characteristic curves of centrifugal pumps working as turbines in different specific speeds. *Exp. Therm. Fluid Sci.* **2008**, *32*, 800–807. [CrossRef]
33. Singh, P.; Nestmann, F. An optimization routine on a prediction and selection model for the turbine operation of centrifugal pumps. *Exp. Therm. Fluid Sci.* **2010**, *34*, 152–164. [CrossRef]
34. Carravetta, A.; Fecarotta, O.; Golia, U.M.; La Rocca, M.; Martino, R.; Padulano, R.; Tucciarelli, T. Optimization of Osmotic Desalination Plants for Water Supply Networks. *Water Resour. Manag.* **2016**, *30*, 3965–3978. [CrossRef]
35. Pugliese, F.; De Paola, F.; Fontana, N.; Giugni, M.; Marini, G. Performance of vertical-axis pumps as turbines. *J. Hydraul. Res.* **2018**, *56*, 482–493. [CrossRef]
36. Rossman, L.A. *Epanet 2 User's Manual*; National Risk Management Research Laboratory Office of Research and Development, U.S. Environmental Protection Agency: Cincinnati, OH, USA, 2000.
37. Carravetta, A.; Del Giudice, G.; Fecarotta, O.; Ramos, H. PAT Design Strategy for Energy Recovery in Water Distribution Networks by Electrical Regulation. *Energies* **2013**, *6*, 411–424. [CrossRef]
38. Carravetta, A.; Del Giudice, G.; Fecarotta, O.; Ramos, H.M. Energy Production in Water Distribution Networks: A PAT Design Strategy. *Water Resour. Manag.* **2012**, *26*, 3947–3959. [CrossRef]
39. Clark, C.O. Storage and the Unit Hydrograph. *ASCE* **1943**, *110*, 1419–1446.
40. Del Giudice, G.; Padulano, R. Sensitivity Analysis and Calibration of a Rainfall-Runoff Model with the Combined Use of EPA-SWMM and Genetic Algorithm. *Acta Geophys.* **2016**, *64*, 1755–1778. [CrossRef]
41. McCuen, R.H. *A Guide to Hydrologic Analysis Using SCS Methods*; Prentice-Hall, Inc.: Upper Saddle River, NJ, USA, 1982; ISBN 0133702057.
42. McCuen, R.H.; Wong, S.L.; Rawls, W.J. Estimating urban time of concentration. *J. Hydraul. Eng.* **1984**, *110*, 887–904. [CrossRef]
43. Carravetta, A.; Conte, M.C.; Fecarotta, O.; Ramos, H.M. Evaluation of PAT performances by modified affinity law. *Procedia Eng.* **2014**, *89*, 581–587. [CrossRef]
44. Galántai, A. The theory of Newton's method. *J. Comput. Appl. Math.* **2000**, *124*, 25–44. [CrossRef]
45. Price List of Public Works. *Reg. Campania* **2016**. Available online: http://www.regione.campania.it/regione/en/topics/price-list-of-public-works (accessed on 19 December 2019).
46. Caprari, S.P.A. Modena, Italy. Available online: https://www.caprari.it/prodotti (accessed on 19 December 2019).
47. Novara, D.; Carravetta, A.; McNabola, A.; Ramos, H.M. Cost Model for Pumps as Turbines in Run-of-River and In-Pipe Microhydropower Applications. *Water Resour. Plan. Manag.* **2019**, *145*, 04019012. [CrossRef]